Journal of the Korean Physical Society, Vol. 52, No. 6, June 2008, pp. 1814∼1817

Ultrahigh-Vacuum-Compatible Diffractometer for Soft X-ray Scattering

J.-S. Lee, B. H. Seung, T.-Y. Khim, H. Jang, K.-T. Ko, B.-G. Park, J.-H. Park and K.-B. Lee
eSSC and Department of Physics, Pohang University of Science and Technology, Pohang 790-784

J.-Y. Kim*
Pohang Accelerator Laboratory and Department of Physics, Pohang University of Science and Technology, Pohang 790-784

(Received 12 December 2007)

We report on the development and the performance of a new instrument for soft X-ray scattering experiments. A ultrahigh- vacuum-compatible two-circle diffractometer was realized by mounting two differentially pumped rotary platforms on top of a cylindrical vacuum chamber. The concentric rotations of the detector and sample are driven by externally-mounted motors and gears. The vacuum chamber itself was designed to accommodate the instruments for surface treatment and *in-situ* film growth. A special cryo-system was also designed to allow changing the sample temperature from 8 K to 480 K. During measurements, a magnetic field of ±1500 Oe can be applied by using an electromagnet along all directions in the scattering plane. The synchronous rotation of the electromagnet with that of the sample is provided by using a separate rotary driver. All functions of the experimental setup have been extensively tested by measuring the ferromagnetic property of the CoFe/IrMn exchange-biased thin film and the antiferromagnetic ordering of $LaSr_2Mn_2O_7$.

PACS numbers: 61.10.-i, 07.85.Jy, 71.27.+a, 75.70.-i
Keywords: X-ray diffraction, X-ray reflectivity, Magnetic scattering

I. INTRODUCTION

Resonant X-ray scattering (RXS) has been used as a useful technique to investigate the spin and the orbital structures of magnetic materials. In particular, it has been also demonstrated in the hard X-ray region that the RXS measurement around the resonant photon energy uniquely provides element-specific, as well as spectroscopic information [1–4]. But soft X-rays are preferred to hard X-rays in RXS studies of magnetic materials. Most magnetic materials are composed of $3d$ transition metals or rare earths and their magnetic properties are largely determined by $3d$ electrons ($3d$ transition metals) or $4f$ electrons (rare earths) at valence states, which are not accessible by direct dipole transitions from K edges ($3d$ transition metals) or L edges (rare earths) in the hard X-ray region [5]. For $3d$ transition metals (rare earths), dipole transitions to the $3d$ ($4f$) valence state are allowed by $2p$ ($3d$) electrons, which correspond to L (M) absorption edges and they all lie in the soft X-ray region of $500 - 1800$ eV. That is to say, resonant soft X-ray scattering (RSXS) measurements can give information on the spin and the orbital structures in a more direct manner than RXS in the hard X-ray region. In addition, soft X-rays have wavelengths of a few nanometers, which agree well with the length-scale of artificial magnetic superstructures, such as magnetic multi-layers and dot-arrays [6–8]. Therefore, RSXS is also very useful to study the collective behavior or magnetic coupling of magnetic superstructures and sometimes it can be made very sensitive to the interface by using a judicious design of multilayers [9]. Thus, the development of RSXS techniques would open up new avenues for studies, ranging from charge, orbital and spin ordering effects in transition metal compounds to the magnetic properties of magnetic multilayers and nano-dot arrays.

From a technical point of view, however, the RSXS setup is far more difficult, because the strong absorption by air requires a diffractometer working at least in a high vacuum environment. Furthermore, the technique is rather surface-sensitive due to the enhanced photon absorption in the vicinity of the resonance energy, which may require *in-situ* surface treatment. Besides, the measurements at cryogenic temperatures can suffer from the formation of additional layers of residual gas. Therefore, an ultrahigh-vacuum (UHV) condition is sometimes inevitable for RSXS measurements, which is not easy to achieve.

Nevertheless, enormous efforts to develop a suitable diffractometer working in UHV have been made by several research groups [10–12]. The aforementioned potentials of RSXS have also led us to develop a versa-

*E-mail: masson@postech.ac.kr; Fax: +82-54-279-1599

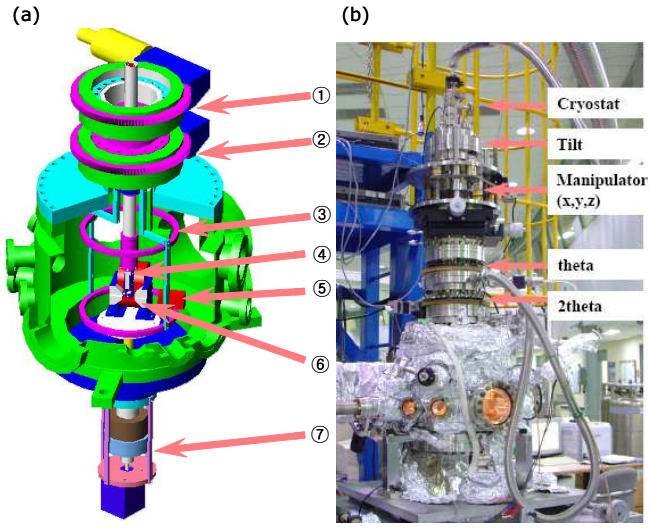

Fig. 1. (color online) (a) Three-dimensional drawing of the diffractometer: ① − ② DPRPs for $\theta - 2\theta$ rotations, ③ A parallel slit for alignment, ④ sample holder, ⑤ detector housing, ⑥ − ⑦ the electromagnet and its rotary driver. (b) Photograph of the scattering chamber showing the $\theta - 2\theta$ angle, manipulator, tilt and cryostat.

tile UHV-compatible two-circle diffractometer accompanying instruments for standard surface treatment. In the following, the details are described and the results of initial measurements are presented.

II. INSTRUMENT DESIGN

To meet the UHV requirement, we designed a cylindrical vacuum chamber and adopted two differentially pumped rotating platforms (DPRPs) as a two-circle goniometer as shown in Figure 1. The goniometer drives the rotation of the sample (θ) and the detector (2θ) inside the chamber. Both DPRPs are concentrically mounted on top of the chamber such that the scattering geometry is horizontal. During their assembly, the offset and tilt between them were carefully checked up and shown to be less than 0.05 mm and 0.01°, respectively. They can be ignored when we consider the horizontal beam size of 0.5 mm at the sample position and the large acceptance angle of the detector. The scattering vector is defined as $Q = 4\pi \sin\theta/\lambda$ and the wavelengths of soft X-ray are larger than those of hard X-rays by orders, which ensures a sufficient Q resolution with an angular acceptance of the detector as large as 0.1°. The rotations of both DPRPs are driven individually by two stepper motors and worm gears, resulting in an angular resolution of 0.005°. With this design, the full angular range of ±180° for the sample rotation is available. The angular range of the detector rotation is about ±170°, which is limited only by the size of the detector.

The diameter and the height of the vacuum chamber are 350 mm and 310 mm, respectively. The sizes are

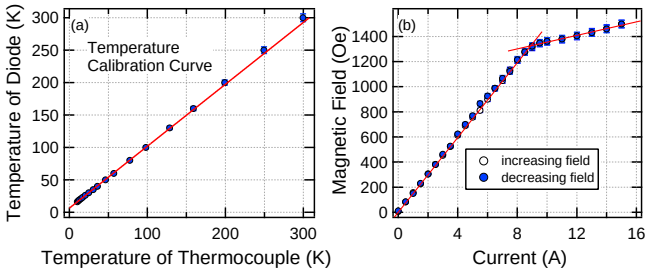

Fig. 2. (color online) (a) Temperature calibration curve. (b) Magnetic field at the center of the gap. Solid lines are guides for the eye.

determined to ensure a sufficiently large arm length for the detector mount and the ports of the chamber are configured to allow the alignment of the sample and the detector with Laser or X-ray. It was also designed to accommodate the instruments for the standard surface treatment and the *in-situ* film growth, such as evaporators, ion-sputterer, thickness monitor and low-energy electron- diffraction analyzer. After the initial baking for two days, an ultimate pressure of 1×10^{-10} Torr was reached. Usually, an UHV as low as 10^{-10} Torr is obtained just after overnight baking.

An open-cycle cryostat was designed to control the sample temperature. It allows heating up to 480 K with a heater and cooling down to 8 K with liquid He. The temperature is measured with an E-type thermocouple, which guarantees enough sensitivity even at cryogenic temperatures. It was also calibrated with a factory-calibrated Si diode, as shown in Figure 2(a). At present, a horseshoe-shaped electromagnet with an iron yoke and a gap of 12 mm is available. The magnet is mounted on a carrousel, where the rotation is driven by a motorized rotary feedthrough from the bottom flange. The magnetic field can be applied in all directions parallel to the scattering plane. It was calibrated *ex situ* before the installation. As shown in Figure 2(b), the maximum magnetic field is 1500 Oe and the remanent magnetic field is confirmed to be as low as 1 Oe at the center of the gap.

The precise alignment of all components is crucial for the performance of the instrument. First of all, the rotation axis of the detector should be placed in the photon beam path and aligned so as to be perpendicular to it. It is accomplished by adjusting two stages of the chamber support and is checked by using two parallel slits, which are also placed in the rotation stage of the detector in opposite directions. Then, the rotation axis of sample shaft is aligned with that of the detector by adjusting the tilt stages on top of the XY-stage. Lastly, the surface of the sample is placed at the rotation center of the detector by adjusting the XY-stage and it is checked by using a hole passing through the center of the sample shaft. Additionally, the alignment of the crystal axis can be done manually by using two degrees of freedom, χ

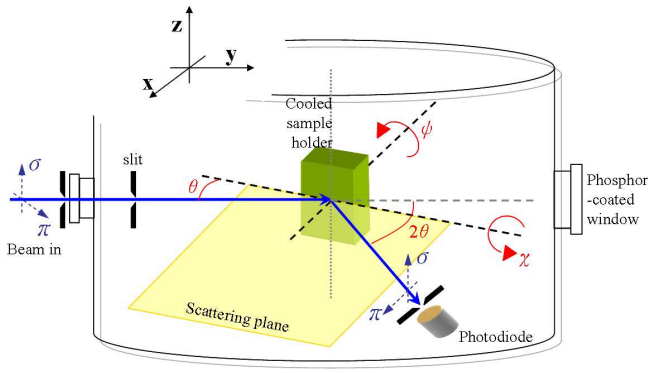

Fig. 3. Schematic drawing of the diffractometer.

and ψ, prepared on the sample holder. The definition of these angles is denoted in Figure 3.

In the present stage of development, the scattered beam is detected by using a Au/GaAsP Schottky photodiode and a slit with a size of 0.5 mm is placed in front of the detector. The Q-resolution can be controlled by changing the size of this slit. The typical current is about 1 μA in the direct beam, which decreases to 0.1 pA at high scattering angles.

III. INITIAL EXPERIMENTAL RESULTS

All functions of the setup were tested successfully and the initial experiments were carried out at the 2A Magnetic Spectroscopy Beamline of Pohang Light Source (PLS). The photon source of the beamline is an elliptically polarized undulator, which supplies a highly brilliant photon beam in the range of 120 – 1800 eV with the polarization tunable from linear to circular. During all measurements described below, the photon energy resolution was set to be 0.3 eV in order to obtain a sufficient photon intensity. The beam intensity was monitored by measuring the photo-current of a gold mesh in front of the diffractometer and the scattered beam intensity was normalized to it.

1. Soft X-ray Resonant Reflectivity

As the first test, we investigated the magnetic property of a well characterized bilayer of $Co_{84}Fe_{16}/Ir_{20}Mn_{80}$ by measuring the resonant reflectivity with circularly polarized soft X-rays. In this system the ferromagnetic (FM) layer of $Co_{84}Fe_{16}$ is exchange-biased by the antiferromagnetic (AFM) layer of $Ir_{20}Mn_{80}$ below the Néel temperature (T_N) of the AFM layer. The phenomenon, exchange bias (EB), is manifested by a shift of the hysteresis loop of the FM layer [13].

Figure 4(a) shows the Q_z dependence of the reflected intensity at the Co L_3-edge (778.1 eV). The oscillation

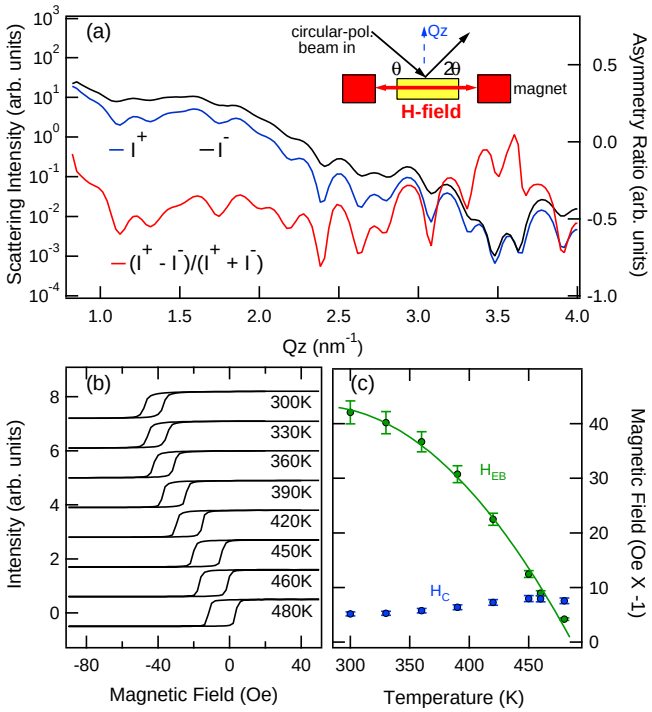

Fig. 4. (color online) (a) The specular reflectivity at the Co L_3 edge. (b) Temperature dependence of M vs. H curves. (c) Temperature dependences of H_{EB} and H_C, where the solid line is a guide for the eye.

corresponds to the thickness of FM layer. The magnetization direction is flipped to be parallel (I^+) and antiparallel (I^-) to the photon helicity vector at each data point. The asymmetry ratio, $\mathcal{R} = (I^+ - I^-)/(I^+ + I^-)$, is also shown in the same figure. It is well known that the ratio is proportional to the magnetization and we can measure the magnetic hysteresis curve by recording the reflected intensity upon changing the magnetic field [14–17]. The hysteresis curves in Figure 4(b) were obtained by using this method. Since the EB field (H_{EB}) above T_N will disappear, we can estimate the T_N of the IrMn layer by extrapolating it as shown in Figure 4(c). The resultant value is 490 K, which agrees well with the previous result [18].

2. Soft X-ray Resonant Diffraction

As the second example, we present the experimental result of soft X-ray resonant diffraction on the $LaSr_2Mn_2O_7$ (LSMO) single crystal. It is well known that LSMO shows A-type AFM spin ordering along the c-axis below a T_c of 170 K [19–21]. The diffraction peak corresponding to this spin ordering was successfully measured by using the newly developed soft X-ray diffractometer. The inset of Figure 5 shows the ordering peak measured at 12 K. For this measurement, linearly polarized soft X-rays with a photon energy of 644 eV (Mn

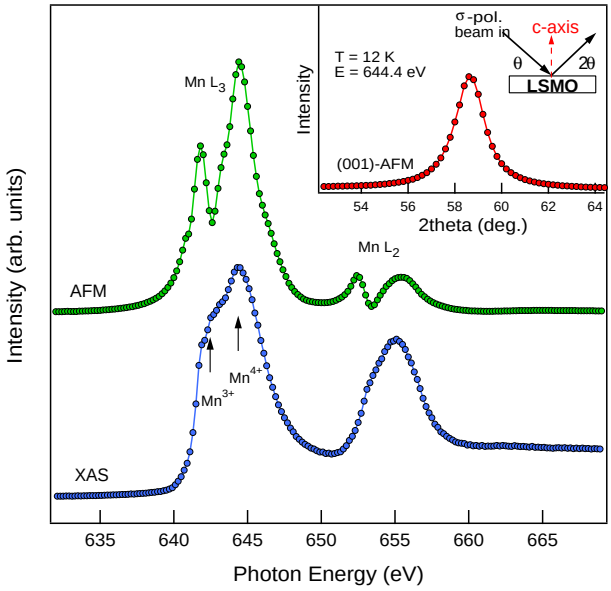

Fig. 5. (color online) Comparison of X-ray absorption spectroscopy (XAS) and energy profile of the AFM ordering (001) peak. The arrows indicate Mn^{3+} and Mn^{4+} sites. Inset: θ-2θ scan of the AFM ordering (001) peak at 12 K.

L-edge) were used. This figure also shows the energy profile of the ordering peak, which was measured upon changing the photon energy while fixing the scattering vector Q at this ordering by adjusting the scattering angle at the same time. This type of measurement can give us spectroscopic information on the contribution of each electronic state to the overall spin ordering. It was obtained with a single scan without noticeable noise. The overall line shape is identical with that of a previous work [19]. The comparison with the X-ray absorption spectrum shows that the separation of two different charge states is far better in the energy profile spectrum, which indicates that the energy profile measurement at around the resonant energy will provide us with an opportunity to study the magnetic ordering with site specificity.

IV. SUMMARY

We have developed a versatile UHV-compatible soft X-ray diffractometer. Its high performance and reliability have been confirmed by conducting soft X-ray scattering experiments on two representative magnetic systems, a $Co_{84}Fe_{16}/Ir_{20}Mn_{80}$ bilayer thin film and a $LaSr_2Mn_2O_7$ single crystal.

ACKNOWLEDGMENTS

This work was supported by grants from Korean Government (MOST and MOEHRD) through the X-ray/particle-beam Nano-characterization Program, the Korea Research Foundation Grant No. KRF-2007-313-C00249 (Basic Research Promotion Fund) and the BK-21 program. Experiments at the PLS were supported by POSTECH and MOST.

REFERENCES

[1] K. Namikawa, M. Ando, T. Nakajima and H. Kawata, J. Phys. Soc. Jpn. **54**, 4099 (1985).
[2] D. Gibbs, D. R. Harshman, E. D. Isaacs, D. B. McWhan, D. Mills and C. Vettier, Phys. Rev. Lett. **61**, 1241 (1988).
[3] M. Blume and D. Gibbs, Phys. Rev. B **37**, 1779 (1988).
[4] M. Imada, A. Fujimori and Y. Tokura, Rev. Mod. Phys. **70**, 1039 (1998).
[5] W. Neubeck, C. Vettier, K.-B. Lee and F. de Bergevin, Phys. Rev. B **60**, 9912 (1999).
[6] K.-Y. Kim, D.-H. Kim, S.-C. Shin and C.-Y. You, J. Korean Phys. Soc. **45**, 1598 (2004).
[7] S.-B. Choe, D.-H. Kim and S.-C. Shin, J. Korean Phys. Soc. **40**, 421 (2002).
[8] W. S. Yun, J. Choi, G.-B. Cha, S. Cho and S. C. Hong, J. Korean Phys. Soc. **49**, 1020 (2006).
[9] Ş. Smadici, P. Abbamonte, A. Bhattacharya, X. Zhai, B. J. A. Rusydi, J. N. Eckstein, S. D. Bader and J.-M. Zuo, Phys. Rev. Lett. **99**, 196404 (2007).
[10] M. Sacchi, C. Spezzani, P. Torelli, A. Avila, R. Delaunay and C. F. Hague, Rev. Sci. Instrum. **74**, 2791 (2003).
[11] J. Grabis, A. Nefedov and H. Zabel, Rev. Sci. Instrum. **74**, 4048 (2003).
[12] P. D. Hatton, S. B. Wilkins, T. A. W. Beale, T. K. Johal, D. Prabhakaran and A. T. Boothroyd, J. Synchrotron Rad. **12**, 434 (2005).
[13] W. H. Meiklejohn and C. P. Bean, Phys. Rev. **102**, 1413 (1956); W. H. Meiklejohn, J. Appl. Phys. **33**, 1328 (1962).
[14] N. Ishimatsu, H. Hashizume, S. Hamada, N. Hosoito, C. S. Nelson, C. T. Venkataraman, G. Srajer and J. C. Lang, Phys. Rev. B **60**, 9596 (1999).
[15] D. Haskel, G. Srajer, J. C. Lang, J. Pollmann, C. S. Nelson, J. S. Jiang and S. D. Bader, Phys. Rev. Lett. **87**, 207201 (2001).
[16] D. R. Lee, S. K. Sinha, D. Haskel, Y. Choi, J. C. Lang, S. A. Stepanov and G. Srajer, Phys. Rev. B **68**, 224409 (2003).
[17] J. B. Kortright and S.-K. Kim, Phys. Rev. B **62**, 12216 (2000).
[18] M. Ali, C. H. Marrows, M. Al-Jawad, B. J. Hickey, A. Misra, U. Nowak and K. D. Usadel, Phys. Rev. B **68**, 214420 (2003).
[19] S. B. Wilkins, P. D. Hatton, M. D. Roper, D. Prabhakaran and A. T. Boothroyd, Phys. Rev. Lett. **90**, 187201 (2003).
[20] Y. Wakabayashi, Y. Murakami, I. Koyama, T. Kimura, Y. Tokura, Y. Moritomo, Y. Endo and K. Hirota, J. Phys. Soc. Jpn. **72**, 618 (2003).
[21] S. Di Matteo, T. Chatterji, Y. Joly, A. Stunault, J. A. Paixao, R. Suryanarayanan, G. Dhalenne and A. Revcolevschi, Phys. Rev. B **68**, 024414 (2003).